BEAR Electrostatic Analyzer: Description and Laboratory Results

DOUGLAS W. POTTER, HUGH R. ANDERSON, JOSEPH R. OLSON

Science Applications International Corporation
13400B Northup Way, Suite 36, Bellevue, Washington 98005

3 January 1990

The Electrostatic Analyzer (ESA) measured the intensity of charged particles returning to the BEAR payload during flight on 13 July 1989. These particles form part or all of the current that returns to the payload to neutralize the charge ejected with the beam. By measuring the return flux with high time resolution, we can study the physics of charging processes. However, the need for high time resolution and sufficient statistics to make a good measurement make design of an appropriate instrument difficult. We solved the major problems and built an instrument with one microsecond time resolution and adequate energy resolution and response.

To support flight measurements, we made a series of measurements in a large plasma chamber at the University of Maryland. The measurements indicate that under most conditions, the level of charging can be determined quite accurately by the Electrostatic Analyzer.

INTRODUCTION

The *geometric factor* of a particle spectrometer is the ratio of the counting rate of the detecting device to the incoming particle intensity in physical units, typically particles/sec-cm^2-ster-eV. The rate must be large enough to pass sufficient particles within the appropriate counting interval to be statistically significant yet low enough to not saturate the detector at its maximum counting rate, typically on the order of 10 MHz. Above the maximum counting rate, the detector typically produces the maximum rate; then, as the input increases still higher, the output drops to zero.

For BEAR, we wanted to get high time resolution to allow examination of the rapid charging process. With the charging process expected to occur on a time scale the order of microseconds or shorter and with a beam pulse only 50 microseconds long, we wanted the time resolution to be one microsecond. With the considerations above, this gives a very small window for accurate measurements. A counting rate of 1 MHz is one count in a microsecond, not really enough to be statistically significant. At ten times that, the detector saturates.

Unfortunately, no theory is available to accurately predict the extremes of intensity. In fact, small changes in assumptions about the nature of the expected environment make changes in the expected intensity of several orders of magnitude. It did appear however, that with most estimates, it would require a very large detector to get a significant number of counts in a microsecond. Since physical space was limited, we elected to make the geometric factors as large as possible within the physical constraints. We reasoned that even if the estimates of high intensity were accurate, it is better to saturate the detector and know that a signal is there than get no signal at all. With limited telemetry (and limited processing capability), we developed a time sampling scheme that called for *one microsecond samples* during and shortly after the pulse, then longer samples to cover most of the interpulse period of 200 milliseconds.

The *energy range* should cover the maximum expected charging potential and overlap the Langmuir probe instrument at the low end. The trade off on energy resolution is that the wider the range, the higher the geometric factor and the lower the number of channels needed to cover a given energy range. A narrower range gives more information on the actual energy. We selected an *energy resolution of 23%*. To avoid convolving time and energy dependence it is absolutely necessary to hold the *selected energy constant* during a given beam pulse cycle. This also helps if there are not enough counts to be statistically significant in one microsecond; we can add together samples until we do get enough counts. Ideally we would use many spectrometers, each of fixed energy, to cover the energy range of interest. Unfortunately limited resources precluded this, so the energy selected by each of the five spectrometers steps after sampling before each new beam pulse. Two detectors cover each of the two species, positive ions and electrons. One of the two covers the range 20-300 eV, the other 200-3000 eV. The fifth spectrometer is a retarding potential analyzer that measures the integral flux above the selected energy.

INSTRUMENTATION

The instrument envelope is a rectangular case 11" x 7" x 10" plus a small top section. Particles are admitted through apertures in the front face. A lining of conetic alloy reduces the magnetic field inside to <10% of the external value.

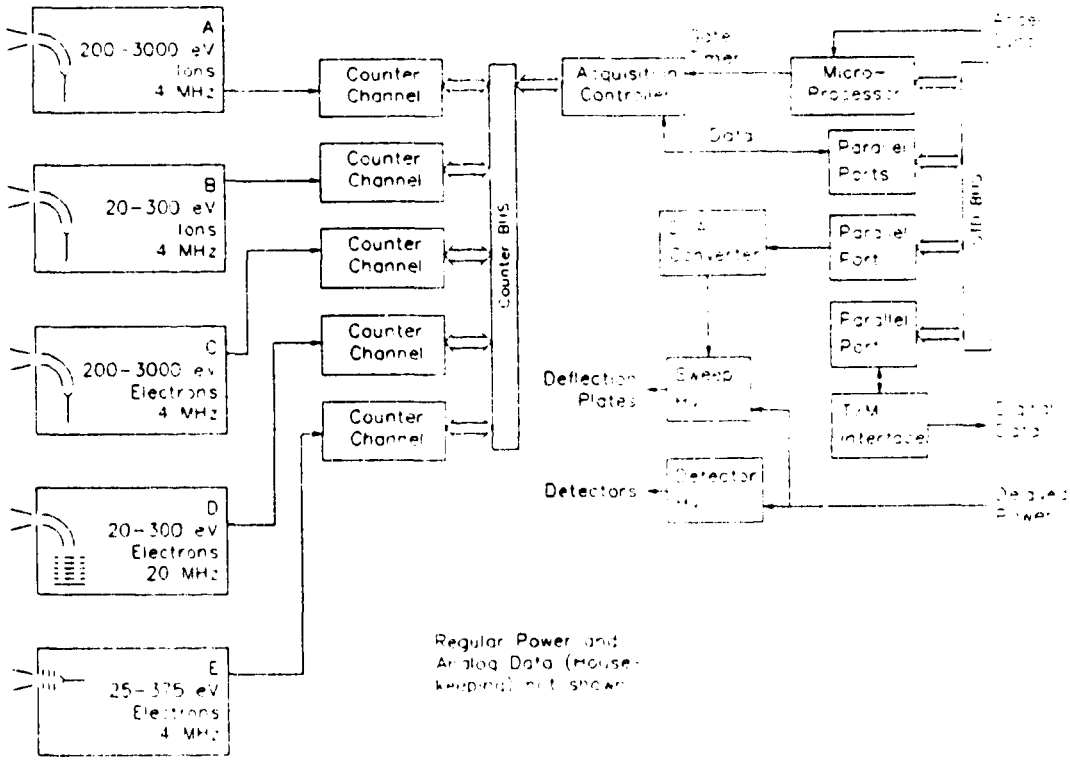

Figure 1. ESA Block Diagram.

BEAR ESA Description

Figure 1 is a functional block diagram. There are four curved plate analyzers, two each for electrons and ions. One of each species covers 20-300 eV, the other covers 200-3000 eV. The plates are sections of spheres using 90 degree deflection angle. By focussing a long entrance slit onto the short exit slit, this geometry allows a large geometric factor. The fifth channel is a retarding potential analyzer (RPA) that covers the range 25-375 eV. The geometric factor of the deflection analyzers is about $0.01E$ [cm^2-ster] with E the center energy of the passband, and the factor of the RPA is 0.01 [cm^2-ster] with all energies above the selected threshold accepted. Using the RPA partially overcomes the problem of not looking at all energies on each beam pulse.

All but the low energy electron channel D use a conventional channel electron multiplier (Galileo channeltron) and a 4 MHz Amptek preamplifier/discriminator. The low energy electron analyzer uses a focussed mesh electron multiplier made by Johnston Labs and a 50 MHz preamplifier/discriminator made by Modern Instrumentation Technology. All multipliers run in the pulse counting mode.

The accelerator sync pulse (prefire pulse), which comes 448 microseconds before the beam-on (rf) pulse, triggers data collection. The microprocessor initializes each of the counter channels and arranges for them to collect data. As Figure 2 shows, two microseconds before the rf pulse, the ESA starts collecting data. First it collects counts in 150 one microsecond long sample gates, then in a variety of longer gates up to one millisecond. The 60 microsecond wide rf pulse represents the time when the rf acceleration is on in the accelerator. Under ideal conditions, the actual pulse comes up to full output 10 microseconds after the rf pulse starts, then ends at the end of the rf pulse.

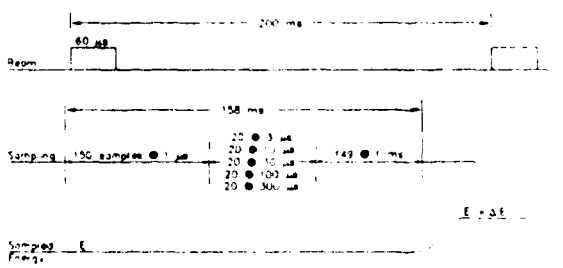

Figure 2 ESA Data Sampling Scheme.

The energy that the analyzers sample is constant for each beam cycle, then steps to the next higher energy for the next beam pulse. In flight, the steps are logarithmically spaced 23% apart - it takes 14 steps to cover the energy range. For most of the laboratory data, we used a mode with 10% spaced steps - which takes 29 steps to cover the energy range.

The Ground Support Equipment (GSE) operates the ESA separate from the BEAR payload by simulating the power and telemetry interface to the instrument and providing the sync signals in lieu of the accelerator. A fiber optic link and isolation power transformer connect elements of the GSE so that the ESA can operate at a potential elevated from laboratory ground.

The GSE uses a PC-AT as a controller and to display and record data from the ESA. This PC generates spectral figures, displays numerical data, and records data on hard disk and tape cassette for later analysis. Figure 3 is a schematic of both the data collection cycle and our typical data display. Note that energy increases towards the front of the plot.

The GSE could also accept data from the telemetry system and display it in real time using the same software as during standalone operation. This allowed us to monitor the behavior of the flight instrument during integrated tests with the entire payload, and to study data promptly after the flight and during laboratory tests.

TEST AND CALIBRATION

Most of the spectrometer calibration was done with spectrometer units outside the ESA. The fast time sampling is not needed for these measurements, and the separate spectrometers can be mounted and rotated in the electron and ion beams of the SAIC calibration system. The experimental results agree well with the calculated response. The calculated response [Morse, 1989] is an expansion of Gosling *et al.* [1984].

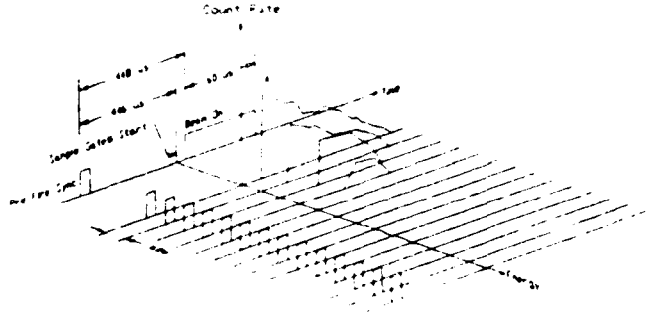

Figure 3. Schematic of GSE Data Display.

OBSERVATIONS

To help characterize the instrument's response to various charging levels, we performed experiments in a large (2m D x 4m) plasma chamber at the University of Maryland (Figure 4). A plasma source in a smaller chamber at one end used 50 eV electrons from a hot filament to ionize nitrogen gas. This filled the main chamber with plasma of density 10^3 to $3x10^5$ cm^{-3}. A langmuir probe furnished with the chamber measured the density. External field coils nulled the geomagnetic field (within 10%) while a second set of coils applied an axial field up to 30 gauss. Most of our measurements were with the geomagnetic field nulled and an axial field of 0.5 gauss.

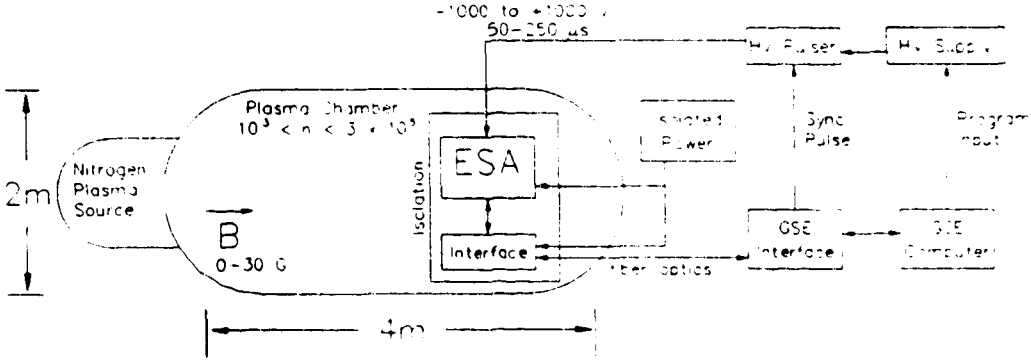

Figure 4. Experimental Setup at the University of Maryland. The ESA can be rotated so that the magnetic field is parallel or perpendicular to the apertures.

We suspended the ESA on the axis of the chamber about 1 meter from the end opposite the plasma source. Signal connections through optical fiber and a power transformer kept the instrument isolated from the chamber walls (laboratory ground). For most measurements the ESA either faced away from the source so that detected particles moved parallel to the magnetic field or faced the chamber side wall so that detected particles moved perpendicular to the field.

Through a triggered switch we applied voltage pulses of various magnitudes up to 1000 volts of both polarities to the instrument while varying the plasma density. The switch either clamped the ESA at ground potential or at the power supply potential with rise and fall times < 100 nanoseconds. The pulse length was either 50 or 250 microseconds.

We emphasize that this particular setup does not accurately mimic the situation in space with an ejected beam because the pulse amplitude is a controlled potential, not a current. Thus these laboratory experiments investigate how the ESA senses a known potential under various conditions, not what that potential is as a function of current to the ESA. Of course the presence of chamber walls does not mimic space either. The dimensions of the chamber were large compared with debye length and electron gyro radius, but small compared with ion gyro radius. The range of plasma densities did cover that expected during the BEAR flight. As a matter of fact the ionospheric density during flight ranged from 1 to 3 x 10^3 /cm^3, the low end of the laboratory range.

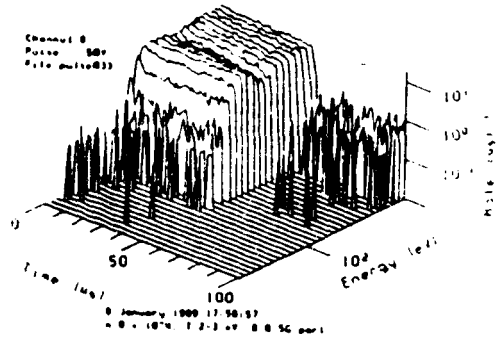

Figure 5. Electron spectrum during a positive pulse of 50 V, parallel orientation.

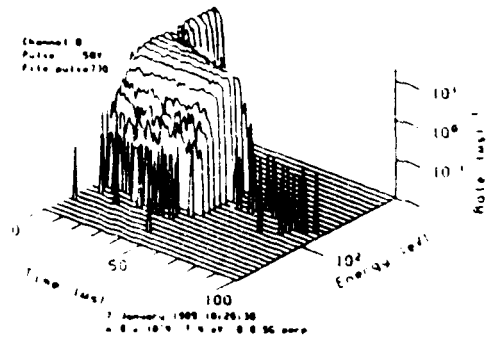

Figure 6. Electron spectra from applied potential of 50V, perpendicular orientation.

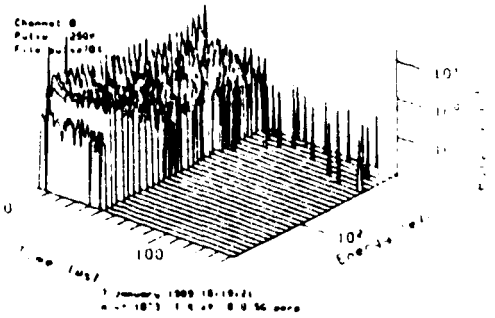

Figure 7. 20-300 eV spectrum from an applied pulse of 250V

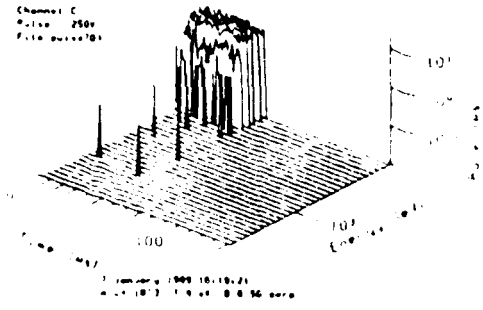

Figure 8. 200-3000 eV Spectrum from a 250 V pulse at plasma density < 10^3

Figure 5 shows a 20-300 eV electron spectrum for orientation parallel to the field and potential pulse amplitude 50 V. Note the fairly square response to the pulse in the lower energy channels, while at the higher energies, there is relatively little response. The square response may be somewhat misleading as the maximum count rate of 17 MHz is the apparent maximum for this channel (D). The trace on the leading edge of the peak corresponds to 78 eV. The trace immediately behind it is 70 eV

Figure 6 shows the same situation except that the orientation of the ESA is perpendicular to the field instead of parallel. The response is similar to the parallel case except that there is a notch behind the energy that corresponds to the applied potential of 50 V. This is a typical distinction between parallel and perpendicular geometry. The traces at the top of the front of the peak are the 78 and 70 eV channels as in Figure 5.

Figure 7 shows the response to a pulse of higher potential but with lower background plasma density. Because the count rate is lower, the detector is in no danger of saturating. The spectrum drops off sharply at the energy that corresponds to the pulse potential of 250 V. The trace at the top energy corresponds to 300 eV, the next lower trace corresponds to 272 eV.

Figure 8 is the same conditions as Figure 7 except that the spectrum is of the 200-3000 eV channel instead of the 20-300 eV channel. The trace across the front face of the pulse is 294 eV.

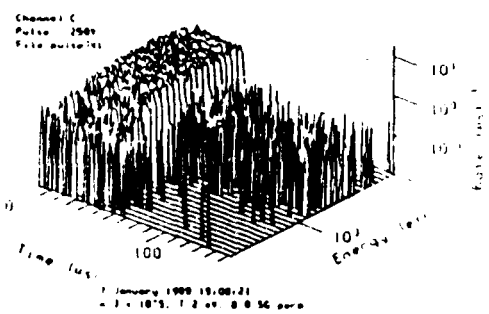

Figure 9. 200-3000 eV electron spectrum for plasma density $3x10^5$, pulse potential 250 V.

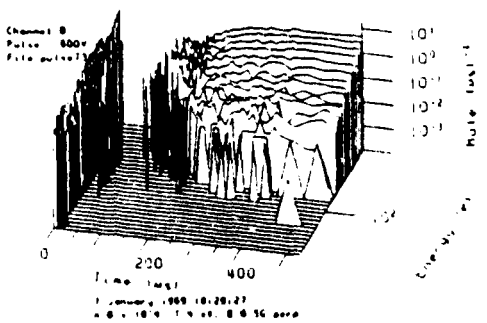

Figure 10. Electron spectrum from a 600 V pulse, plasma density $8x10^4$. Data are from Channel D.

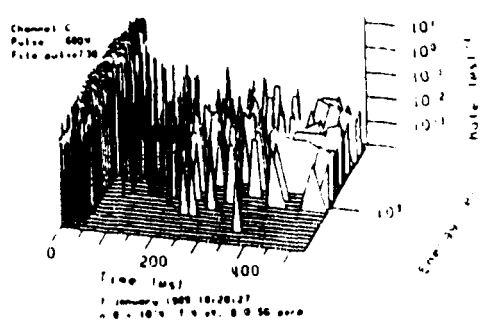

Figure 11. Same as Figure 10 except Channel C (200-3000 eV electrons).

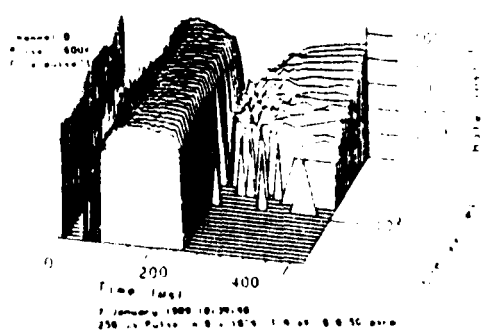

Figure 12. Electron Spectrum from a 250 microsecond long pulse.

Figure 9 is the same conditions as Figure 8 except that the plasma density is much higher at $3x10^5$. The high energy tail of electrons above the energy corresponding to the applied potential makes determination of the charging level difficult.

Figure 10 and Figure 11 show the response to a 600V pulse, plasma density $8x10^4$; the two figures show channels D and C, high and low energy electrons. As Figure 10 is the 20-300 eV spectrum and the orientation is perpendicular, it shows the notch behind the energy corresponding to the pulse potential. Note that the time axis extends for 500 microseconds instead of the 100 microseconds in the previous figures.

Figure 12 is exactly the same conditions except that the pulse is 250 instead of 50 microseconds long. The 50 microsecond long pulse was not long enough to reveal the rather noticeable notch in the response at about 30-70 microseconds. At least in the lab, the spectral response is dynamic for longer than 50 microseconds.

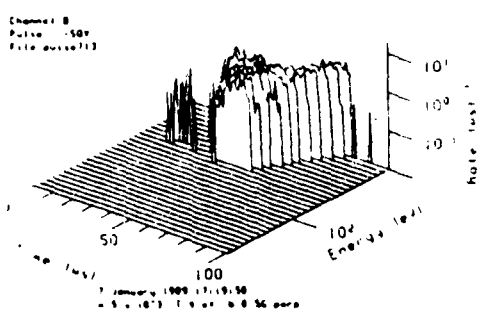

Figure 13. 20-300 eV ion spectrum from applied pulse of -50 V.

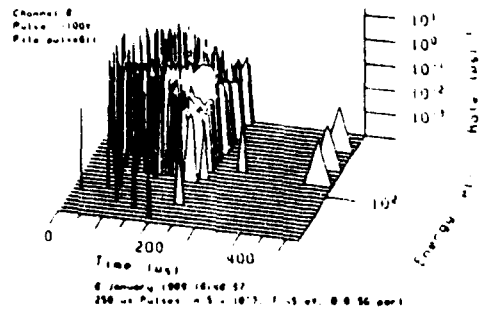

Figure 14. Ion spectrum from a -100 V 250 microsecond pulse.

Figure 13 is the *ion* response to an applied pulse of -50 V. The trace on the front of the pulse corresponds to 53 eV. The response takes much (relatively speaking) longer than the corresponding electron response. Still the edge of the spectrum corresponds to the charging potential. Figure 14 is the ion spectrum from a 100 V pulse of length 250 microseconds. Because of the parallel geometry, the spectral edge only gets to its expected value after the first 50 microseconds.

Figure 15 shows that the edge of the electron spectrum follows the applied potential extremely well over a wide range of conditions. Figure 16 shows that the ion response is similar except that at parallel geometries and low potentials, the ions do not respond in sufficient time to reach the energy that corresponds to the pulse amplitude.

CONCLUSIONS

The ESA responded satisfactorily over the entire range of plasma densities and applied voltages. Although the electron multipliers ran at their maximum rate with the higher densities, this did not obscure the correspondence between spectra and voltage pulse amplitude.

The spectra of collected particles extend from the lowest energy channel to the value corresponding to the amplitude of applied voltage. Above this energy the spectra dropped sharply. An exception was that at the highest plasma densities a tail of high energy electrons appeared in Channel C, making the spectral edge less sharp. In the case of perpendicular motion the spectra are continuous during the first several microseconds to the energy corresponding to the pulse, just as in the case of parallel motion. Thereafter a notch appears in the spectra at energies a little below the edge.

The electron spectra developed rapidly after the (positive) voltage pulse was applied. Ion spectra, on the other hand, required some tens of microseconds to develop after a (negative) pulse was applied. In some cases the ion spectra did not fully develop during 50 microseconds. The longer 250 microsecond pulses revealed fuller development.

These ion observations were similar for both parallel and perpendicular motion with respect to the magnetic field B. However, the delay in ion development was more pronounced for parallel motion.

Figure 15 and Figure 16 show that we can infer the voltage applied to the ESA from the spectra it observes.

Acknowledgements. L. Millonzi and G. Kroft of SAIC/Las Vegas designed and fabricated the digital electronics. Randy Dockter, also of that office, designed and wrote the software for both the instrument microprocessor and the GSE. Aeronautical Testing Service of Arlington, Washington designed and fabricated the mechanical package.

We are indebted to Drs. John Antoniades and Rodney Greaves of the University of Maryland for helping us make measurements in the chamber. In particular, Dr. Greaves spent most of weekend, including Saturday night, helping make measurements. We especially want to thank Don Cobb, project manager; Morrie Pongratz, project scientist and the rest of the BEAR Project office for being all we could wish in a sponsor. Their continued support makes this work possible.

Contract 9-X58-7568P-1 from Los Alamos National Laboratory supports this work.

REFERENCES

Gosling, J. T., M. F. Thomsen, and R. C. Anderson. A cookbook for determining the essential transmission characteristics of spherical section electrostatic analyzers. LANL Report LA-10147-M. 1984.

Morse, D. L. Bear ESA instrument spectrometer response, calibration, and modelling. SAIC Report SAIC/NW-89-DLM-996-50. 1989

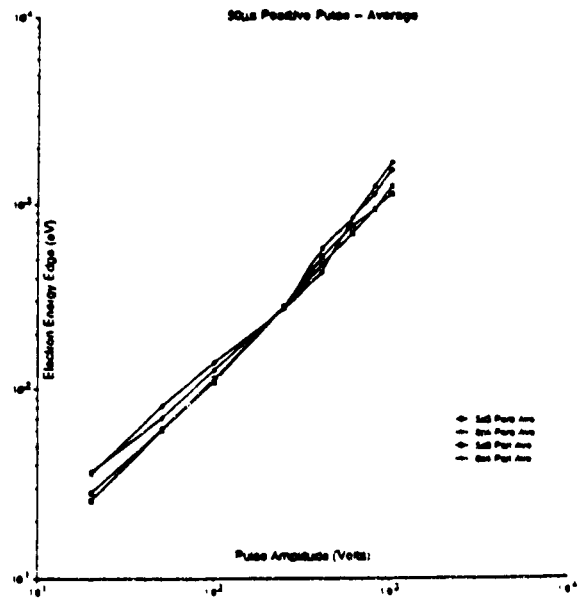

Figure 15. Spectral edge vs. applied pulse potential for electron response to positive charging.

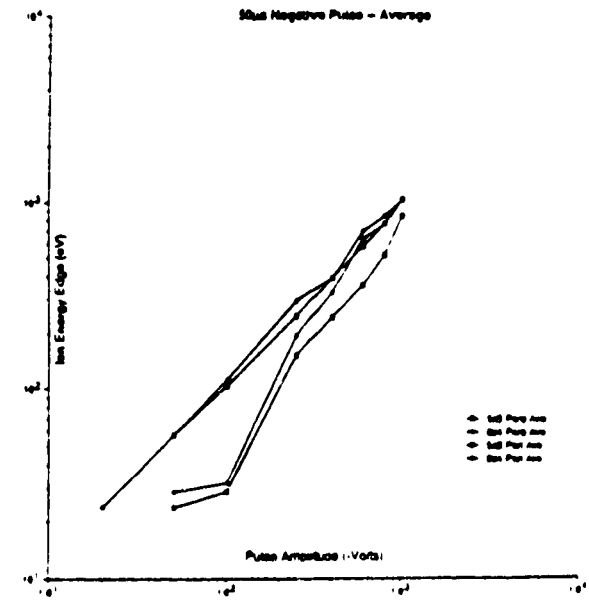

Figure 16. Ion response to negative charging